Phosphorescent Oxygen Sensors Based on Nanostructured Polyolefin Substrates

ARTICLE *in* ANALYTICAL CHEMISTRY · JANUARY 2010

Impact Factor: 5.64 · DOI: 10.1021/ac902406w · Source: PubMed

9 AUTHORS, INCLUDING:

Ross N Gillanders
University of St Andrews
7 PUBLICATIONS **143** CITATIONS
SEE PROFILE

Olga Arzhakova
Lomonosov Moscow State University
34 PUBLICATIONS **135** CITATIONS
SEE PROFILE

Joe P Kerry
University College Cork
297 PUBLICATIONS **6,546** CITATIONS
SEE PROFILE

Dmitri B Papkovsky
University College Cork
153 PUBLICATIONS **3,165** CITATIONS
SEE PROFILE

analytical chemistry

Article

pubs.acs.org/ac

Oxygen-Sensitive Phosphorescent Nanomaterials Produced from High-Density Polyethylene Films by Local Solvent-Crazing

Claudio Toncelli,[†] Olga V. Arzhakova,[‡] Alla Dolgova,[‡] Aleksandr L. Volynskii,[‡] Nikolai F. Bakeev,[‡] Joe P. Kerry,[§] and Dmitri B. Papkovsky*,[†]

[†]University College Cork, Biochemistry Department, Cavanagh Pharmacy Building, Cork, Ireland

[‡]Department of Polymer Chemistry, Moscow State University, Leninskie Gory, Moscow, Russian Federation

[§]Department of Food Science and Nutrition, University College Cork, Cork, Ireland

ABSTRACT: Discrete solid-state phosphorescent oxygen sensors produced by local solvent-crazing of high density polyethylene films are described. The simple spotting of dye solution followed by tensile drawing of the polymer substrate provides uniform nanostructures with good spatial control, effective encapsulation of dye molecules, and quenchability by O_2. The dye−polymer composite sensors prepared using toluene as a solvent and stabilized by annealing at high temperature, show moderate optical signals, near-optimal sensitivity to O_2 (RSD at 21 KPa 1.9%), and reproducible phosphorescence lifetime readings. Calibration experiments performed over 0−25 kPa O_2 and 10−30 °C temperatures ranges reveal linear Stern−Volmer plots and temperature dependences and minimal effect of humidity on sensor calibration. The high degree of lateral and in-depth homogeneity of these O_2-sensitive materials was confirmed by high-resolution atomic force and wide-field optical microscopy, including 2D and 3D phosphorescence lifetime imaging.

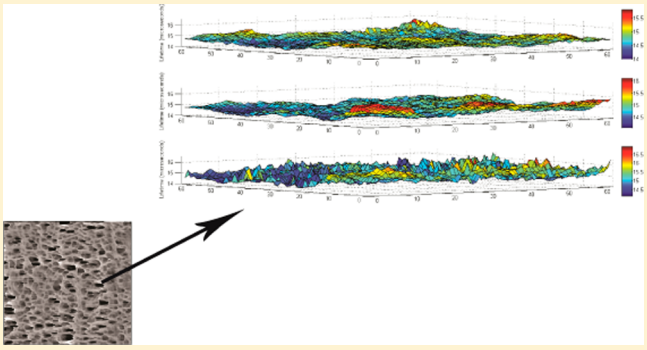

Solid-state phosphorescent sensors for molecular oxygen (O_2) are gaining popularity in many areas, including industrial process control, environmental monitoring, biological detection, medicine, and food packaging.[1−3] The advantages of such materials and techniques include their nonchemical, reversible response to O_2 and the ability to perform contactless noninvasive measurements,[4] unlike the traditional methods such as Winkler titration and Clark-type electrodes.[2] Such O_2-sensitive materials are usually produced by encapsulation of phosphorescent dye molecules in an O_2-permeable polymeric or inorganic matrix and arranging the latter in the form of a thin film or coating.[5] The type of encapsulation matrix determines sensor sensitivity (Stern−Volmer quenching constant), response time, and other operational characteristics.[6] Polymer selection is determined by the reporter dye used, targeted O_2 range, and application requirements. Common encapsulation media for O_2 sensors include polystyrene, silicones and ormosils, fluorinated polymers, plasticized polyvinylchloride, and some other polymers.[2,6,7]

Nondestructive control of residual O_2 in packaged products (e.g., O_2-sensitive foods, beverages, pharmaceuticals, and electronic products) is important, as nonoptimal O_2 levels may lead to rapid degradation of enclosed products through oxidation, enzymatic reactions, and microbial spoilage.[3] A sensor for packaging should satisfy a number of special requirements, particularly high robustness and reproducibility, low cost (i.e., ca. $\leq$ 1 p per cm^2), simple composition, and manufacturing process.[8] Sensor safety and shelf life in contact with the packaged material should be adequate, especially for food products.[4] Another crucial issue is integration of O_2 sensor technology, both the material and fabrication method, in standard packaging processes. Ideally the sensor should be introduced into the packaging without major process modifications.[4] From these viewpoints, the existing materials, polymers and fabrication technologies used in modern optical O_2 sensors do not satisfy all the requirements of large-scale applications, such as packaging.

Polyethylene (PE) and polypropylene (PP) are common and cheap polymers widely used in packaging laminates, particularly as heat-sealable inner layer exposed to food, together with a layer (or several layers) of barrier material(s) facing the other side.[9] However, PE and PP are not very common in fabrication of O_2 sensors, due to their limited compatibility with the established O_2-sensitive dyes and encapsulation methods. Sensor fabrication usually relies on casting or printing of polymeric 'cocktails' in organic solvent,[10] adsorption, polymerization/curing, sol−gel method,[11] nano and microprecipitation,[12] and extrusion.[13]

Solvent crazing in a physically active liquid environment (PALE) has been suggested for incorporation in polymeric

Received: December 16, 2013
Accepted: January 14, 2014
Published: January 14, 2014

   dx.doi.org/10.1021/ac404072z | *Anal. Chem.* 2014, 86, 1917−1923

substrates of physically or thermodynamically incompatible additives such as metals (a two-step process with introduction of silver ions and their subsequent reduction to metallic silver), titanium dioxide nanoparticles,[14,15] and organic dyes.[16,17] This method usually involves tensile drawing of the polymer substrate (film or fiber) in a suitable additive-containing solvent system, which leads to the development of specific nanoporous structures with overall volume porosity of up to 55−60%, pore dimensions ranging from 5−15 nm, and narrow pore size distribution. The process is controlled by the nature of the polymer (initial structure, degree of crystallinity, and organization of crystalline phase in semicrystalline polymers) and deformation conditions (tensile strain, applied stress, nature of PALE, strain rate, etc.). The content of incorporated additive depends on the overall porosity and its concentration in feed solution.[18]

Solvent crazing of high-density polyethylene (HDPE) and PP films have recently been applied to fabrication of phosphorescent O_2 sensors.[16] When the polymer substrate was drawn in the PALE (*n*-heptane), the dye molecules penetrated into the formed nanoporous structure, got finely dispersed, and enclosed in it with low aggregation and self-quenching, thus producing phosphorescent PE/PP films with usable optical signals and response to O_2. Optionally, the open-pore structure of the formed solvent-crazed polymer can be healed by annealing at elevated temperatures or further drawing.[16]

So far, impregnation of polymers by solvent crazing has been conducted mainly as a batch process,[19] which requires substantial amounts of PALE and the dye. On the other hand, packaging applications favor the use of discrete sensors (5−10 mm in diameter), which can be applied on polymeric substrates with high flexibility and spatial control.

In this study, we hypothesized that local deposition of dye-containing PALE on small regions of polymer film, by simple spotting, can help mitigate the undesirable consequences of the batch process. In this case, tensile drawing should produce discrete O_2 sensor spots on the film and (in the future) directly on the packaging material (online). This approach compatible with standard printing technologies also reduces the usage of toxic and flammable organic solvents and valuable sensor material (phosphorescent dye). Here we demonstrate the production of discrete O_2 sensors by local spot-crazing of HDPE films in PALE-containing Pt(II)-tetrabenzoporphyrin (PtBP) dye and perform spectroscopic and functional characterization of such materials. By measuring phosphorescent lifetime and intensity signals in air and nitrogen atmosphere, we assessed the effects of the main parameters on sensor behavior and optimized the fabrication process, including the solvent, strain rate, film thickness, dye concentration, and further annealing and rinsing with solvents. Optimised sensors then underwent more detailed morphological and spectroscopic characterization by high-resolution AFM andoptical imaging and looking at their full O_2 calibrations under different temperatures (10, 20, and 30 °C) and environmental conditions (dry/humid/wet). Phosphorescence lifetime imaging was also applied to examine lateral and in-depth microheterogeneity of the discrete solvent-crazed HDPE film sensors, both in 2D and 3D.

EXPERIMENTAL SECTION

Materials. We used commercial blown HDPE films, 25 μm thick from DSM/SABIC (Netherlands) and 80 μm thick (Russia), with crystallinity 48−56% (according to Mettler DSC analyzer, Switzerland) and T_m = 129 °C. Pt(II)-meso-tetrabenzoporphyrin (PtBP) was from Frontier Scientific, analytical grade 2-butanone, toluene, anisole, dimethylsulfoxide, and glacial acetic acid were from Sigma-Aldrich. O_2 and N_2 gases, 99.9% were from Irish Oxygen (Ireland).

Solvent-Crazing Procedure. A strip of HDPE film (3.0 × 5.0 cm) was clamped at the edges in a custom-made drawing device.[14] Twenty microliters of PtBP solution in the appropriate solvent were applied with a micropipet to the center of the film, which was then immediately stretched at a constant rate of 6 mm min^{-1} to the desired tensile strain (100−200%). The resulting solvent-crazed film was wiped to remove residual solvent, dried in air, then released and allowed to shrink. The process (shown schematically in Scheme 1) makes

Scheme 1. Scheme of Sensor Production by Local Solvent-Crazing

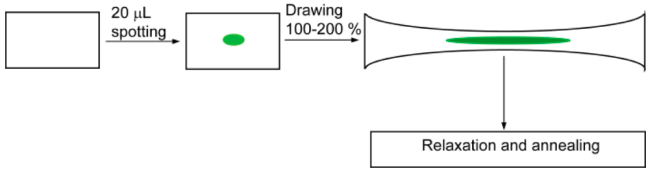

it possible for dye molecules to penetrate into the polymer and to be immobilized within the formed nanoporous structure.[16] Optionally, solvent-crazed films were annealed at 100 °C for 10 min to heal the nanopores and/or rinsed with organic solvent.

Spectroscopic Characterization of Sensors. For screening and optimization experiments, phosphorescence intensity and lifetime signals were measured from the solvent-crazed sensors placed on white support, using a hand-held Optech instrument (Mocon, Minneapolis). Each sensor zone was measured three times in different locations, and average values and standard deviations were calculated. Sensor calibrations were performed with a Firesting instrument (PyroSciences GmbH, Germany) operating with a 1 mm fiber-optic probe, under standard manufacturer's settings. Sensors were measured without white support. Phase shift readings were converted into lifetime values according to the following equation: $\tau = \tan(\theta)/(2\pi\vartheta)$, where τ is the lifetime (sec), θ is the phase shift (rad), and ϑ is the modulation frequency (4.0 kHz). Standard O_2/N_2 gas mixtures (0 − 21 kPa O_2) produced by precision gas mixer (LN Industries SA, Switzerland) were pumped through a glass vial containing a solvent-crazed O_2 sensor which was interrogated with the Firesting probe. The vial was submerged in a circulating water bath (Julabo), and calibration gases were passing through a loop of stainless steel tubing also submerged in the bath.

Microscopic Measurements. AFM imaging experiments were carried out on a Femtoscan microscope (Advanced Technologies Center) in tapping and contact modes. Commercial silicons NSG11 (spring constant 11.5 N m^{-1}, resonant frequency 255 kHz) and CSG01 (spring constant 0.03 N m^{-1}, resonant frequency 9.8 kHz) were used for tapping and contact scanning mode, respectively (both from NTMDT, Russia). The scan rate was typically 1.8 Hz, and the number of lines −512.

Wide-field optical imaging was performed on a system consisting of an inverted microscope Axiovert 200 (Zeiss) with Plan Neofluar 40x/1.3 oil immersion objective, pulsed

dx.doi.org/10.1021/ac404072z | Anal. Chem. 2014, 86, 1917−1923

Table 1. Phosphorescent Characteristics of O_2 Sensors Produced in Different Solvents[a]

solvents	relative permittivity (ε)	T_b (°C)	τ_o (zero O_2) (μs)	τ_q (21 kPa O_2) (μs)	I_0 (zero O_2) (a.u.)	I_q (21 kPa O_2) (a.u.)
heptane	1.9	98	47.75 ± 0.29	9.02 ± 0.37	2100 ± 400	700 ± 60
toluene	2.4	110.6	49.44 ± 0.11	14.24 ± 0.22	10700 ± 600	2650 ± 150
anisole	4.3	153.7	49.06 ± 0.09	12.78 ± 0.24	5100 ± 600	1400 ± 100
anisole/acetic acid 70/30	4.3/6.2	153.7/118	48.77 ± 0.45	13.51 ± 0.26	6400 ± 900	1700 ± 200
toluene/acetic acid 70/30	2.4/6.2	110.6/118	48.74 ± 0.15	12.25 ± 0.16	11100 ± 500	2400 ± 300
toluene batch process	2.4	110.6	48.68 ± 0.22	10.80 ± 0.21	7800 ± 1500	1700 ± 90

[a]Samples were produced using 80 μm HDPE, 200% elongation rate, 0.20 mg mL^{-1} dye concentration, and 20 μL volume. Annealing was at 100 °C for 10 minutes. Measured on white support with Optech instrument at 24 °C.

Table 2. Effects of the Main Process Parameters of Localized Crazing in Toluene on the Characteristics of HDPE Sensors[a]

parameter	specification	τ_q (zero O_2) (μs)	τ_o (21 kPa O_2) (μs)	I_q (zero O_2) (a.u.)	I_0 (21 kPa O_2) (a.u.)
annealing	untreated	46.12 ± 0.43	18.43 ± 1.12	15800 ± 800	5900 ± 900
	annealed	49.42 ± 0.11	14.23 ± 0.22	10700 ± 600	2650 ± 150
elongation (%)	100	48.92 ± 0.08	11.15 ± 0.16	8300 ± 500	1700 ± 500
	150	48.69 ± 0.51	12.29 ± 0.17	7100 ± 1200	1750 ± 150
	200	49.42 ± 0.11	14.24 ± 0.22	10700 ± 600	2650 ± 150
thickness (μm)	25	47.90 ± 0.38	10.46 ± 0.15	4400 ± 250	1100 ± 100
	200	49.42 ± 0.11	14.24 ± 0.22	10747 ± 550	2650 ± 150
dye concentration (mg mL^{-1})	0.1	48.66 ± 0.39	12.66 ± 0.31	6000 ± 1200	1600 ± 150
	0.15	49.18 ± 0.14	13.83 ± 0.30	6500 ± 400	1700 ± 60
	0.20	49.42 ± 0.11	14.24 ± 0.22	10700 ± 600	2650 ± 150
optimal sensor	annealed	48.45 ± 0.06	13.13 ± 0.17	9100 ± 1300	2200 ± 200
PtBP in PS	n/a	51.99 ± 0.10	21.15 ± 0.09	14000 ± 2100	4700 ± 300

[a]Unless specified otherwise, sensors were made from 80 μm thick HDPE using 20 μL of dye solution 0.20 mg/mL, 200% elongation rate, and annealing at 100 °C for 10 min. Measured on white support with Optech instrument at 24 °C.

excitation module (590 nm LED), gated CCD camera (LaVision BioTec), excitation 595/40 nm and emission 780/60 nm filter cube, and incubation chamber with O_2 and temperature control (PeCon).[20] Frame time in fluorescence and differential interference contrast (DIC) modes was 100−150 ms. Phosphorescence lifetime imaging (PLIM) settings (Delay T, snapshot mode) at 21 kPa O_2 were pulse width 10 μs, repetition time 170 μs, gate time 10 μs, delay time 0−100 μs, 11 images; frame time 100 ms, no binning. At 1 kPa O_2, the settings were pulse width 10 μs, repetition time 190 μs, gate time 20 μs, delay time 0−120 μs, 11 images, frame time 100 ms, no binning. Lifetimes were calculated from monoexponential fits with time window and offset adjustment.

Confocal microscopy was performed on a TCSPC-PLIM system (Becker & Hickl, Germany) based on an upright microscope Axio Examiner Z1 (Zeiss) with oil immersion objective Neofluar 100×/1.3 for DIC images or LD C-Apochromat 40×/1.1 for phosphorescence, heated stage with motorized *Z*-axis control, and a DCS-120 confocal scanner (Becker & Hickl) with two excitation and two emission channels.[21] A 405 nm picosecond diode laser (Becker & Hickl), connected to the DCS-120 scanner with an optical fiber was used for the excitation. Emission was detected with a 750−810 nm bandpass filter and R10467U-40 photon counting detector (Hamamatsu) connected to the scanner and controlled by TCSPC hardware.[22] DIC images were recorded with a digital camera Nikon D5100 connected to the microscope.

RESULTS AND DISCUSSION

Optimization of Fabrication of Discrete Sensors. For semicrystalline polyolefins such as HDPE and PP, which have complex structure with amorphous and crystalline phases, tensile drawing in PALE is accompanied by profuse cavitation and formation of nanometer pores. With increasing tensile strain, volume porosity of the polymer tends to increase to about 52−55% and level off when stretching reaches ∼200%. The high porosity is accommodated in the interlamellar spaces and provided by progressive lamellar separation upon stretching. In the presence of PALE, amorphous interlamellar regions are plasticised by the liquid, which enhances the efficiency of lamellar separation and concomitant cavitation and aids the development of high porosity.[23] The size and density of the formed nanopores are determined by the nature of the PALE.

In the original study on solvent-crazed O_2 sensors,[16] batch process was used in which the polymeric substrate was strained, being fully submerged in heptane (crazing environment). In the current study, we aimed to achieve local crazing under a small drop of solvent, as shown in Scheme 1. Here, heptane having relatively high evaporation rate and limited solubility for PtBP dye was not quite appropriate. Toluene looks more promising for local solvent crazing, since its higher boiling point should prevent rapid evaporation of small amounts of solvent (20 μL of drops) during film drawing; so does anisole, which shows an even higher boiling point, good solubility of the dye (>1 mg mL^{-1}). In order to limit contact area of the drop of solvent with HDPE substrate, mixtures of toluene and anisole with hydrophilic acetic acid were also tested. All these solvents have relatively low toxicity (class III of ICH solvent guide list), which is essential for food applications.

The sensors produced by localized solvent-crazing of HDPE films looked clearly colored with the dye and slightly opaque. Their signals were generally lower (∼4-fold for optimized sensors) than for conventional O_2 sensors (e.g., polystyrene coatings on microporous light-scattering support).[24] To increase their phosphorescent signals when measuring with

dx.doi.org/10.1021/ac404072z | Anal. Chem. 2014, 86, 1917−1923

the hand-held phosphorescent detector Optech, the sensors were placed on white support (paper sheet). A comparison of phosphorescent signals of different sensors in air and nitrogen is given in Tables 1 and 2.

The higher signals from sensors produced by spot-crazing in toluene reflect higher degrees of dye encapsulation, which can be attributed to stronger interaction of dye molecules with the polymeric structure.[25] The efficiency of quenching by O_2, reflected by lifetime values in air, was also influenced by the solvent (Table 1). The solvent was also seen to slightly alter the "unquenched" lifetime (and intensity) signals in N_2, likely due to internal quenching or dye aggregation.

Hence, during crazing the solvent creates different microenvironment for the additive[1] and contributes to O_2 diffusion and accessibility of PtBP dye molecules within the polymer matrix. The different structure of cavitated polymers produced by local crazing of HDPE films in different solvents has a marked effect on the brightness and quenching of the resulting sensors. On the basis of this initial screening, toluene was selected as preferred solvent for sensor fabrication. It provides optimal brightness, quenching by O_2, low variability of readings from individual sensors (SD of lifetime values in air and N_2), and robust changes in optical signals in the range of highest practical importance (0−25 kPa O_2).

The sensors produced by local crazing in toluene were also compared with those produced by the batch method. The latter sensors gave significantly lower phosphorescence intensity values in air and nitrogen and higher variability (S.D.) of lifetime values. These results show that local wet crazing is more efficient and produces brighter (partial solvent evaporation and dye concentration) and better quality O_2 sensors. It also reduces exposure to harmful solvent vapors and the amounts of sensor material used (currently 20 μL per spot, but can be smaller).

The effects of other parameters, namely film thickness, tensile strain, dye concentration, annealing, and washing after crazing, are summarized in Table 2. Thus, annealing at elevated temperatures (close to T_m) is known to have a beneficial effect on solvent-crazed O_2 sensors, stabilizing their characteristics and response to O_2.[16] Indeed, we observed enhanced phosphorescent signals, likely due to dissolution of aggregates and/or elimination of internal quenching of the dye. Lifetime and intensity signals in N_2 attained higher values and O_2 quenching was moderately increased. Rinsing sensor films in organic solvent after the annealing step was seen to have little effect on their intensity signals (dye leaching) and response to O_2. This proves (as in our previous observations[16]) that the dye molecules are permanently trapped within the polymer, and nanopores are healed up.

Tensile strain also increased the lifetime and intensity signals (Table 2), probably due to enhanced stress-driven diffusion of the plasticising solvent into the amorphous regions of semicrystalline polymer, thus facilitating the development of nanopores and increasing the overall volume porosity of the sample.[23] Thicker films showed higher intensity signals because the overall intake of the dye is higher, and they are mechanically more stable (better preserve the formed nanopores and prevent contraction after tensile drawing). However, O_2 quenching was higher in thinner films, suggesting that they have less heterogeneous polymer matrix. Higher dye concentration also increased the intensity signal to a maximum (0.20 mg mL^{-1}), after which the dye started to aggregate on the polymer surface.

On the basis of this optimization work, the following conditions were selected for sensor fabrication: 80 μm thick HDPE, 20 μL of 0.20 mg mL^{-1} PtBP in toluene, 200% elongation, and 10 min annealing at 100 °C. Using these conditions, we produced several batches of sensors and measured their mean lifetime and intensity values and SD (Table 2, second last line). Compared to PtBP in polystyrene, solvent-crazed sensors showed higher quenching by O_2, which translates into higher sensitivity of O_2 measurements. Moreover, the SD of lifetime in air and nitrogen was comparable to the former. Lower intensity signals are not a major obstacle for industrial applications: instrument sensitivity can be tuned and sensor signals increased (e.g., by using thicker films, other polymers, or lamination) to achieve the desired measurement performance.

Sensor Characterization. The fine structure of the wet-crazed polymers can be visualized by the atomic force microscopy. Figure 1a shows AFM images of the HDPE film before and after the local crazing by stretching in toluene, and after subsequent annealing.

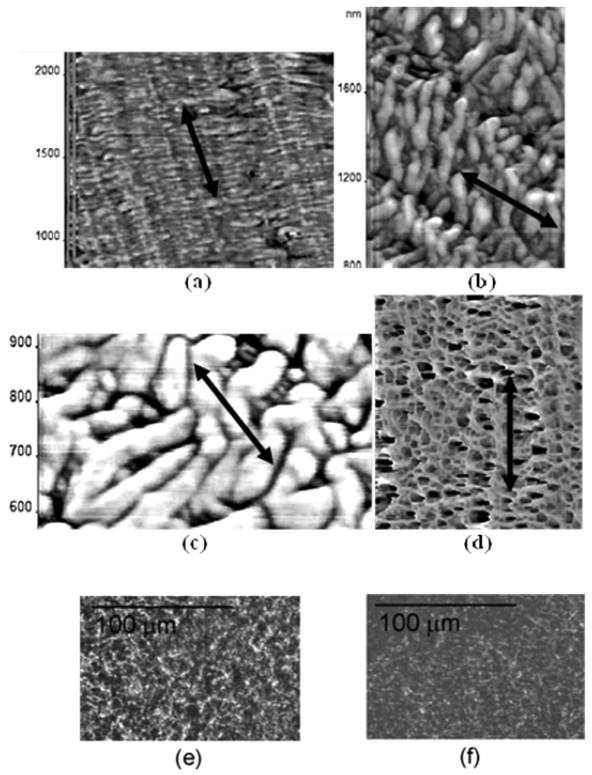

Figure 1. Images of (a) the initial HDPE blown films, (b and c) same film after local solvent-crazing by stretching by 200% and drying under isometric conditions, and (d) film b,c after annealing under isometric conditions produced by AFM (black arrows show the direction of extrusion/stretching), and optical microscopy images of (e) solvent-crazed and (f) dry-stretched polymer at 100× magnification. Samples: HDPE 80 μm, 20 μL of 0.20 mg mL^{-1} dye in toluene, and 200% elongation at room temperature.

The initial film is seen to have the shish-kebab structure characteristic for semicrystalline polymers with well-defined folded-chain crystalline lamellas, whose planes are normally oriented in the direction of melt extrusion. The thickness of each lamella is about 30−40 nm. The amorphous phase is sandwiched between the crystalline lamellas (interlamellar

dx.doi.org/10.1021/ac404072z | Anal. Chem. 2014, 86, 1917−1923

regions). The images of the wet-crazed HDPE film (Figure 1, panels b and c, tensile strain is 200%) show that now the lamellas drifted apart but remained intact and preserved their initial thickness at the same level. The drifted lamellas are connected by thin fibrils of nanometer size separated by pores of the same size. This implies that, upon stretching in PALE, lamellas are separated, and the amorphous phase is organized in thin nanoscale fibrils by the meniscus instability mechanism. Thus, all strain is accommodated in the amorphous phase of the polymer where cavitation and fibrillation occur. The dye-containing solvent easily penetrates the cavitated amorphous phase, and dye immobilization occurs within the weblike fibrillar structure. After the annealing under isometric conditions, the structure appears to be heavily percolated by pores (Figure 1d). However, when the sample is allowed to shrink or annealed free-standing, the porous structure is totally healed and the dye entrapped tightly inside the polymer. Optical images at 100× magnification (bright-field, micrometer scale) also confirm significant changes (degree of "roughness") in the structure of the initial polymer film after local solvent-crazing in toluene (Figure 1, panels e and f).

Operational Performance. For optimized (vide supra) sensors, full O_2 calibrations were performed at three different temperatures, 10, 20, and 30 °C. They showed the anticipated dependences of the phosphorescence lifetime (Chart 1). For

Chart 1. Calibrations, Stern–Volmer Plots, Temperature Dependence, and Dry and Wet Calibrations[a]

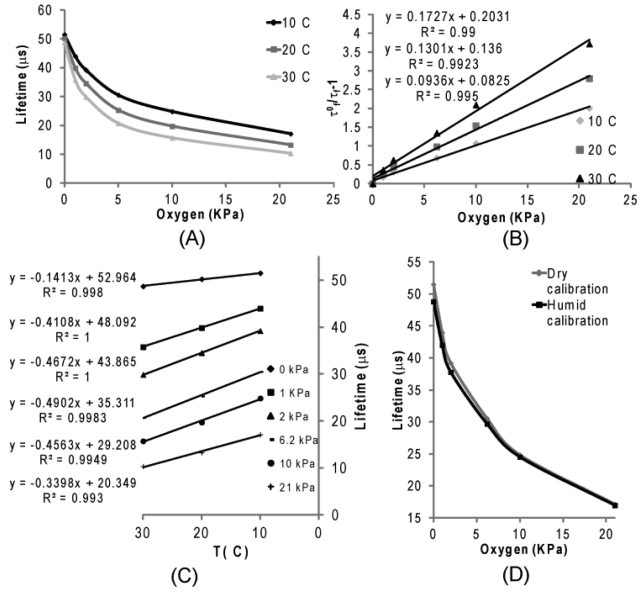

[a](A) Lifetime calibrations for discrete solvent-crazed O_2 sensors in the gas phase at 10, 20, and 30°C. (B) Stern–Volmer plots derived from A with linear fits. (C) Temperature dependence of lifetime at different pO_2. (D) Dry and wet calibrations at 10°C. Measured with Firesting instrument.

dynamic quenching by O_2, lifetime is expected to have the following temperature dependence:[26]

$$\frac{1}{\tau} = k_f^0 + A_{nr}e^{-\Delta E_{nr}/RT} + A_q^0 e^{-\Delta E_q/RT} \quad (1)$$

where k_f^0 is the kinetic constant of luminophore's decay, A_{nr} and A_q^0 are pre-exponential factors of nonradiative and O_2 quenching processes, and ΔE_q and ΔE_{nr} are their activation energies, respectively.

Equation 1, which accounts for all the processes affecting the quenching, describes a general case. However, for the narrow temperature range and three experimental points studied here, the dependence can be fitted satisfactorily with trend lines, as depicted in Chart 1C. These relationships can be used for compensation of O_2 measurements for variation of sample temperature. The local crazed sensors displayed good linearity of their Stern–Volmer plots at all studied temperatures (Chart 1B). This reflects their high homogeneity and allows simple two-point calibration (τ_f^0 and τ_f), unlike many other O_2 sensors which show pronounced heterogeneity originating from the polymer matrix.[1]

The influence of humidity on sensor calibration was small but detectable (Chart 1D). This is consistent with the findings that sensors based on hydrophobic polymers (polystyrene, polyvinylchloride, silicones as well as HDPE) are less influenced by humidity than hydrophilic polymers (e.g., ethyl cellulose, cellulose butyrate acetate).[27] Humidity affects physical characteristics of polymers and quenching behavior of O_2 sensors.[27]

Lifetime signals obtainable from the sensor during the calibration experiments were stable. Under continuous measurement conditions at 21 kPa O_2 signal-to-noise ratio in phase shift mode was less than 0.021 degrees, which translates into an oxygen error of 0.15%. Measurement of O_2 with different sensors from the same batch (see Chart 1 and Table 2) gave a SD in 21 and 0 kPa O_2 of around 0.39 and 0.07, respectively. High stability and batch-to-batch reproducibility of discrete manually produced O_2 sensors reflects robustness of the method. We anticipate that this can be further improved by automation, better control of liquid dispensing, drawing, and annealing.

Wide field (2D) and confocal (3D) fluorescence microscopy were applied to further probe microheterogeneity of the sensors.[16] Distribution of phosphorescence intensity and lifetime signals was analyzed at a different O_2 concentration. Wide-field intensity images show good uniformity of impregnation across solvent-crazed sensor and marked changes in intensity and lifetime when going from 21.0 to 1.0 kPa O_2 (Figure 2, panels A and B).

In phosphorescent imaging, variation of measured signal is generally greater than in macroscopic spot measurements with hand-held readers, due to lower signal-to-noise and more complex signal processing algorithms of the former. However, high uniformity and homogeneity of the sensors are clearly seen on the lifetime images, presented as distribution histograms, cross sections, and 2D surface patterns in pseudocolor scale (Figure 2, panels C–H). No particular lateral patterns or irregularities were visible, so we concluded that on a microscale, the sensors produce uniform signal with variation resembling random noise.

Conversely, changes in O_2 concentration affect the decay curves, reducing the amplitude and increasing steepness at 21 kPa compared to 1 kPa O_2 (Figure 2E).

The uniformity of the sensor material produced by local solvent-crazing was also confirmed by confocal (3D) microscopy using TCSPC-PLIM method. We generated several intensity and lifetime images for different stacks across the film thickness (0, 20, and 40 μm deep) and found that lifetime values were consistent across the film depth and the response to oxygen was uniform (Figure 3, panels A and B).

dx.doi.org/10.1021/ac404072z | Anal. Chem. 2014, 86, 1917–1923

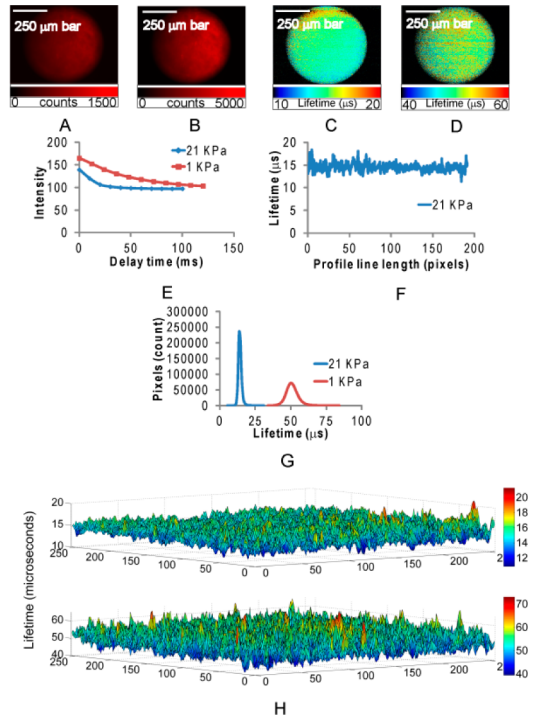

Figure 2. Wide-field imaging of toluene crazed sensors at 40× magnification: (A and B) intensity, (C and D) lifetime signals, and (E) phosphorescence decays at 21.0 and 1.0 kPa O_2. (F) Line profile, (G) distribution, and (H) surface plots of lifetime values for a ROI 256 × 256 pixels (area 28375 μm^2) at 21.0 kPa (top) and 1.0 kPa (bottom) O_2.

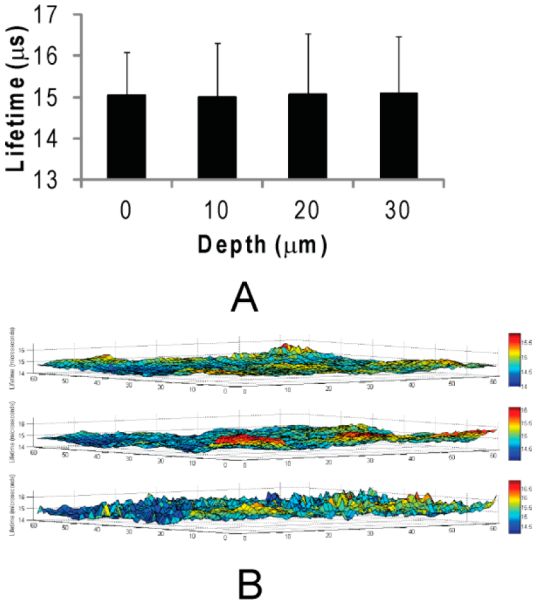

Figure 3. 3D imaging of solvent-crazed sensors by confocal TCSPC-PLIM microscopy. Average lifetime for the entire recorded area at (A) different depths and (B) 2D surface plots for regions 64 × 64 pixels (366 μm^2) at the surface (top), 20 μm (center), and 40 μm (bottom) deep.

Surface maps of the deep layers show a higher variation of the lifetime, likely due to inner filter effect, and weaker phosphorescent signals received by the detector (not shown).

CONCLUSION

Discrete solid-state O_2 sensors based on the commercial HDPE film and PtBP phosphorescent dye were fabricated by local crazing in small drops of toluene. This technology, which is compatible with standard printing and polymer processing (e.g., orientation) technologies, provides simple and easily controlled fabrication of discrete, small-size O_2 sensors with good reproducibility, robustness, and homogeneous distribution of dye molecules across the polymer substrate. It also offers advantages of reduced consumption of the hazardous solvent and valuable phosphorescent dye. The sensors show satisfactory operational performance, simple linear calibrations, and useful range of O_2 concentrations (0–21 kPa). They allow simple integration in large-scale industrial applications and development of "smart" packaging materials and systems for nondestructive control of residual O_2.

AUTHOR INFORMATION

Corresponding Author

*E-mail: d.papkovsky@ucc.ie.

Author Contributions

The manuscript was written through contributions of all authors. All authors have given approval to the final version of the manuscript.

Notes

The authors declare no competing financial interest.

ACKNOWLEDGMENTS

Financial support of this work by the Irish Department of Agriculture, Food and Marine, Grant DAFM 11/F/015, is gratefully acknowledged. Authors wish to thank Dr. R. Dmitriev for the help in imaging experiments.

REFERENCES

(1) Ruggi, A.; van Leeuwen, F. W. B.; Velders, A. H. *Coord. Chem. Rev.* **2011**, *255*, 2542–2554.
(2) Quaranta, M.; Borisov, S. M.; Klimant, I. *Bioanalytical Reviews* **2012**, *4*, 115–157.
(3) Papkovsky, D. B.; Dmitriev, R. I. *Chem. Soc. Rev.* **2013**, *42*, 8700–8732.
(4) Mills, A. *Chem. Soc. Rev.* **2005**, *34*, 1003–1011.
(5) Klimant, I.; Kuhl, M.; Glud, R. N.; Holst, G. *Sens. Actuators, B* **1997**, *38*, 29–37.
(6) Amao, Y.; Okura, I. *J. Porphyrins Phthalocyanines* **2009**, *13*, 1111–1122.
(7) Kamachi, T.; Okura, I. In *Handbook of Porphyrin Science*; Kadish, K. M., Smith, K. M., Guilard, R., Eds.; World Scientific: New Jersey, pp 297–348.
(8) Amao, Y. *Microchim Acta* **2003**, *143*, 1–12.
(9) McKeen, L. W. In *Plastic Films in Food Packaging*; William Andrew Publishing: Oxford, 2013; pp 1–15.
(10) Koren, K.; Hutter, L.; Enko, B.; Pein, A.; Borisov, S. M.; Klimant, I. *Sens. Actuators, B* **2013**, *176*, 344–350.
(11) Chu, C. S.; Lo, Y. L. *Sens. Actuators, B* **2008**, *134*, 711–717.
(12) Kondrashina, A. V.; Dmitriev, R. I.; Borisov, S. M.; Klimant, I.; O'Brien, I.; Nolan, Y. M.; Zhdanov, A. V.; Papkovsky, D. B. *Adv. Funct. Mater.* **2012**, *22*, 4931–4939.
(13) Mills, A.; Lawrie, K.; Bardin, J.; Apedaile, A.; Skinner, G. A.; O'Rourke, C. *Analyst* **2012**, *137*, 106–112.
(14) Volynskii, A. L.; Bakeev, N. F. *Polym. Sci., Ser. C* **2011**, *53*, 35–47.
(15) Volkov, A. V.; Polyanskaya, V. V.; Moskvina, M. A.; Tunyan, A. A.; Zezin, S. B.; Dement'ev, A. I.; Volynskii, A. L.; Bakeev, N. F. *Colloid J.* **2013**, *75*, 40–48.

(16) Gillanders, R. N.; Arzhakova, O. V.; Hempel, A.; Dolgova, A.; Kerry, J. P.; Yarysheva, L. M.; Bakeev, N. F.; Volynskii, A. L.; Papkovsky, D. B. *Anal. Chem.* **2010**, *82*, 466−468.
(17) Volkov, A. V.; Tunyan, A. A.; Moskvina, M. A.; Dement'ev, A. I.; Yaryshev, N. G.; Volynskii, A. L.; Bakeev, N. F. *Polym. Sci., Ser. A* **2011**, *53*, 158−165. Volkov, A. V.; Tunyan, A. A.; Moskvina, M. A.; Volynskii, A. L.; Dement'ev, A. I.; Bakeev, N. F. *Polym. Sci., Ser. A* **2009**, *51*, 563−570.
(18) Rukhlya, E. G.; Litmanovich, E. A.; Dolinnyi, A. I.; Yarysheva, L. M.; Volynskii, A. L.; Bakeev, N. F. *Macromolecules* **2011**, *44*, 5262−5267.
(19) Bucknall, C. B. *Polymer* **2012**, *53*, 4778−4786.
(20) Fercher, A.; Zhdanov, A.; Papkovsky, D. In *Phosphorescent Oxygen-Sensitive Probes*; Springer: Basel, 2012, pp 71−101.
(21) Becker, W.; Bergmann, A.; Biskup, C. *Microsc. Res. Tech.* **2007**, *70*, 403−409.
(22) Haugland, R. P.; Spence, M. T. Z.; Johnson, I. D. *The Handbook: A Guide to Fluorescent Probes and Labeling Technologies*; Molecular Probes: Eugene, OR, 2005.
(23) Volynskii, A. L.; Bakeev, N. F. In *Solvent Crazing of Polymers*; Volynskii, A. L.; Bakeev, N. F., Eds.; Elsevier: Amsterdam, 1995; pp 29−136.
(24) Papkovsky, D. B.; Ovchinnikov, A. N.; Ogurtsov, V. I.; Ponomarev, G. V.; Korpela, T. *Sens. Actuators, B* **1998**, *51*, 137−145.
(25) Makitra, R.; Pyrih, Y.; Sagladko, E.; Turovskiy, A.; Zaikov, G. *J. Appl. Polym. Sci.* **2001**, *81*, 3133−3140.
(26) Badocco, D.; Mondin, A.; Pastore, P. *Sens. Actuators, B* **2012**, *163*, 165−170.
(27) Eaton, K.; Douglas, P. *Sens. Actuators, B* **2002**, *82*, 94−104.